ASHRAE REGION AT LARGE ARC_CAIRO EGYPT
6-8 September 2003, Cairo

Paper No., RAL-3-5

HEAT TRANSFER ENHANCEMENT IN A LATENT HEAT THERMAL STORAGE SYSTEM USING EXTERNALLY FINNED CHANNELS: NUMERICAL AND EXPERIMENTAL STUDY

K. M. EL-SHAZLY, S. A. ABDEL-MONIEM®, E. F. ATWAN,
A. A. ABDEL-AZIZ, AND R. K. ALI©
Mech. Eng. Dept., Faculty of Eng. (Shoubra),, 108 Shoubra St., Cairo, Egypt

ABSTRACT

A numerical and experimental study was carried out to investigate the transient response of a modified latent heat storage system. The proposed system was composed of phase change material (PCM) packed in the spaces between externally finned flow channels. Preliminary modeling for a system containing PCM with simple geometry and flow configuration was carried out either considering the natural convection or the effective thermal conductivity. The natural convection model was based on the solution of the vorticity and energy equations of both the PCM and the working fluid via a finite difference technique with Alternating Direction Implicit method (ADI). The conduction model was adopted based on an effective thermal conductivity (K_{eff}) of the melted zone of the PCM. The results of the natural convection model were utilized in a parametric study to estimate K_{eff} and new correlation was obtained. This correlation was permitted to a modified conduction model to predict the performance of enhanced storage systems with externally finned flow channels at different configurations.

An experimental apparatus was designed and constructed to verify the numerical results. The influences of the working fluid mass flow rate, inlet fluid temperature, initial temperature of the PCM, flow channel pitch and fin configurations on the storage characteristics were investigated. It was found that the storage performance of the plain-channel systems is independent on Reynolds number beyond a value of 300. Also the enhancement in the storage characteristics of the finned channel systems is strongly dependent on the fin pitch and the fin length while it does not depend on the fin thickness. New correlations were obtained for the melted volume ratio and the amount of the heat stored for the finned channel systems as functions of the different operating parameters.

KEY WORDS: Phase change material, thermal energy storage, finned channels

® *Author to whom correspondence should be addressed: E-mail: Sayed_Moneim@ hotmail.com*
© *Ph. D. Student*

1. INTRODUCTION

Thermal energy storage systems may be included in a broad spectrum of applications such as solar energy, off-peak electric energy storage with utilization of the electrically generated heat or coolness during peak demand periods, industrial waste heat utilization, refrigerated cargo transport, building heating and cooling, and greenhouses.

The storage of thermal energy by means of phase-change materials (PCMs) has attractive features over sensible energy storage due to its large storage capacity and nearly isothermal behavior during charging and discharging. The relatively small storage volumes required by PCMs hold the promise of cost and design advantages for large-scale applications and can help to reduce environmental pollution. Efforts to employ PCMs have included a variety of geometries and fluid flow configurations that are designed to provide adequate heat exchanges. The energy storage systems using heat exchangers with different geometries and the solution methods for related phase change problems are reviewed by Ilken and Tokosy [1]. Several fundamental studies are available on heat transfer during melting and solidification of PCMs for systems with plain-flat geometries [2-8].

Generally, phase change energy storage devices suffer from the low thermal conductivity of the PCM and consequently, the decrease in the rate of heat transfer. This can be improved by using a proper heat transfer enhancement technique. There are several methods to enhance the heat transfer in latent heat thermal storage systems (e.g. fins configurations, dispersing high conductivity particles [9, 10], encapsulation of PCM [11-14], bubbles agitation and lessing rings [15]. The use of finned surfaces with different configurations has been proposed by [15-23]. Velraj et al. [15] and Sparrow et al. [16] investigated experimentally different heat transfer enhancement methods for latent heat storage systems using finned tubes. Pandmanabhan and Krishna [17] have also studied the phase change process occurring in a cylindrical annulus in which (i) rectangular, uniformly spaced longitudinal fins, spanning the annulus (ii) annular fins are attached to the outer surface of the inner isothermal tube, while the outer tube is made adiabatic. Eftekhar et al. [18] have experimentally studied the melting of paraffin by constructing a model that consists of vertically arranged fins between two isothermal planes. The photographs of the molten zone indicate that a buoyant flow induced in the neighborhood of the vertical fin causes rapid melting of the solid wax. Smith and Koch [19] have done a theoretical study of solidification adjacent to a cooled flat surface containing fins. The effects of fin conduction parameter and fin dimensions on solidification rate and heat transfer have been studied. Larcox [20] has presented a theoretical model for predicting the transient behavior of a shell-and-tube storage test unit having annular fins externally fixed on the inner tube with the phase-change material on the shell side and the heat transfer fluid flows inside the tube. The numerical results have also been validated with

experimental data for various parameters like shell radius, mass flow rate and inlet temperature of the heat transfer fluid. An analytical study was performed by Yimer and Adami [21] to investigate the effect of various geometrical and thermal parameters on the performance of a PCM thermal storage system. Shell and tube arrangement with longitudinal fins included inside the PCM in the annulus. The use of fins increased both the storage capacity and the melting front penetration and nothing have been mentioned about the optimum number of fins. Velraj et al. [22] have presented theoretical and experimental work for a thermal storage unit consisting of a cylindrical vertical tube with internal longitudinal fins. The results indicated that the enhancement in heat transfer with fins is several folds as compared to the case with no fins.

The main objective of the present study is to investigate the enhancement in the performance characteristics of a PCM thermal storage system using externally finned channels with different configurations. Furthermore, the effective thermal conductivity of the melted PCM is one of the targets of the present numerical analysis. This is accomplished through a parametric study by comparing the results of the natural convection and the modified conduction models.

2. SYSTEM MODELING

In the present analysis two different configurations are considered. The physical models, coordinate systems, solution domains and boundary conditions for the two different configurations are shown in Fig.(1).

The following assumptions are introduced in the present analysis:

1. Thermophysical properties of the PCM may differ in the solid, mushy and liquid phases while they are isotropic and homogeneous in the same phase.
2. The volume change due to the solid-liquid change is negligible.
3. The thermophysical proprieties of the PCM and the working fluid are independent of temperature within the investigation range of the temperature.
4. The heat storage in channel walls is negligible.
5. The used fins are sufficiently thin so that it can be treated as a one dimensional model.

The governing conservation equations are normalized in dimensionless forms by employing the following dimensionless parameters:

$x^* = x/H, y^* = y/H$ dimensionless coordinates x, y

$\tau = \alpha_l \, t/H^2$ dimensionless time

$\theta = \dfrac{T - T_{mp}}{T_{ref} - T_{mp}}$ dimensionless temperature, T_{ref} is the heated surface temperature for the simple model, Fig.(1-a) and T_{ref} is the inlet fluid temperature for the finned channel model, Fig.(1-b).

$u^* = u/u_o$, $v^* = v/u_o$ dimensionless velocities in x and y-directions where, u_o is a reference velocity , $u_o = \alpha_l / H$

$\Psi^* = \Psi/\alpha_l$ dimensionless stream function

$\omega^* = \omega/(\alpha_l/H^2)$ dimensionless vorticity

2.1. Natural Convection Model

The governing equations described by Cao and Faghri [24] and Sakr [2] for a simple adiabatic enclosure with an isothermal heated surface shown in Fig.(1-a) are reduced into dimensionless forms as:

The vorticity equation:

$$\frac{\partial \omega^*}{\partial \tau} + u^* \frac{\partial \omega^*}{\partial x^*} + v^* \frac{\partial \omega^*}{\partial y^*} = Pr\left(\frac{\partial^2 \omega^*}{\partial x^{*2}} + \frac{\partial^2 \omega^*}{\partial y^{*2}}\right) + Gr\, Pr^2 \frac{\partial \theta_{PCM}}{\partial x^{*2}} \quad (1)$$

where, $\omega^* = -\left(\frac{\partial^2 \Psi^*}{\partial x^{*2}} + \frac{\partial^2 \Psi^*}{\partial y^{*2}}\right)$, ψ^* is the dimensionless stream function defined by; $u^* = \frac{\partial \Psi^*}{\partial y^*}$ and $v^* = -\frac{\partial \Psi^*}{\partial x^*}$

The energy equation:

a) for the liquid phase:

$$\frac{\partial \theta_l}{\partial \tau} + u^* \frac{\partial \theta_l}{\partial x^*} + v^* \frac{\partial \theta_l}{\partial y^*} = \frac{\partial^2 \theta_l}{\partial x^{*2}} + \frac{\partial^2 \theta_l}{\partial y^{*2}} \quad (2)$$

b) for the solid phase:

$$\frac{\partial \theta_s}{\partial \tau} = \alpha_s\left(\frac{\partial^2 \theta_s}{\partial x^{*2}} + \frac{\partial^2 \theta_s}{\partial y^{*2}}\right) \quad (3)$$

c) for the mushy phase:

$$\frac{\partial \theta_m}{\partial \tau} = \alpha_m\left(\frac{\partial^2 \theta_m}{\partial x^{*2}} + \frac{\partial^2 \theta_m}{\partial y^{*2}}\right) \quad (4)$$

2.2. The Modified Conduction Model

The energy equation for the PCM utilizing the effective thermal conductivity of the liquid phase in a dimensionless form is;

$$\frac{\partial \theta_{PCM}}{\partial \tau} = \alpha_r\left(\frac{\partial^2 \theta_{PCM}}{\partial x^{*2}} + \frac{\partial^2 \theta_{PCM}}{\partial y^{*2}}\right) \quad (5)$$

where, $\alpha_r = \begin{cases} \alpha_s/\alpha_l & \text{for the solid phase} \\ \alpha_{eff}/\alpha_l & \text{for the liquid phase} \\ \alpha_m/\alpha_l & \text{for the mushy phase} \end{cases}$

2.3. The Enhanced Finned Channels Model

The dimensionless energy equation for the enhanced model with finned channel, shown in Fig.(1-b) is:

i) for the PCM:

$$\frac{\partial \theta_{PCM}}{\partial \tau} = \alpha_r \left(\frac{\partial^2 \theta_{PCM}}{\partial x^{*2}} + \frac{\partial^2 \theta_{PCM}}{\partial y^{*2}} \right) \tag{6}$$

ii) for the working fluid(heat carrier)

$$\frac{\partial \theta_f}{\partial \tau} = -\mathrm{Re}\, \frac{H}{D_H} \frac{\nu_f}{\alpha_l} \frac{\partial \theta_f}{\partial x^*} + 2\,\mathrm{Nu} \frac{H^2}{D_H W} \frac{\alpha_f}{\alpha_l} (\theta_{PCM} - \theta_f) \tag{7}$$

iii) for the fins

$$\frac{\partial \theta_{fin}}{\partial \tau} = \frac{\alpha_{fin}}{\alpha_l} \frac{\partial^2 \theta_{fin}}{\partial y^{*2}} + \frac{k_{PCM}}{k_{fin}} \frac{H}{Z} \frac{\alpha_{fin}}{\alpha_l} \left(\left. \frac{\partial \theta}{\partial x^*} \right|_{right} + \left. \frac{\partial \theta}{\partial x^*} \right|_{left} \right) \tag{8}$$

2.4. The Initial and Boundary Conditions

The storage system is initially at the ambient temperature and the governing equations are subjected to the following boundary conditions:

i-for the natural convection and the modified conduction models

- at the adiabatic surfaces, $\frac{\partial \theta}{\partial n} = 0.0$, where n is a normal vector
- at the isothermal heated surface (at $x^*=0$), $\theta = 1$
- in the natural convection model, for the whole boundaries of the liquid phase $\omega^* = \frac{-3\Psi^*_{w+1}}{(\Delta l^*)^2} + \frac{\omega^*_{w+1}}{2}$, as described in [25] where, $\Delta l^* = \Delta l / H$.

ii- for the enhanced finned channels model

- at the flow channel inlet, $\theta_f = 1$

3. NUMERICAL SOLUTION

The governing equations for the PCM, working fluid and the fins are approximated by using finite difference technique. The formulation utilizes a central difference for the first and the second derivatives. The second upwind finite difference technique is implemented to overcome the non-linearity in energy and the vorticity equations. These result in the following difference equations for the grid notation shown in Fig.(2):

a- for natural convection model

The vorticity at a node i, j in the liquid phase is written in explicit form as:

$$\omega_{i,j}^{*0+1/2}=\omega^{*}_{i,j}\left\{1-\frac{\Delta\tau}{2}\left(\frac{UR+|UR|-UL+|UL|}{2\Delta x^{*}}+\frac{VA+|VA|-VB+|VB|}{2\Delta y^{*}}\right)-\frac{Pr\,\Delta\tau}{(\Delta x^{*})^{2}}-\frac{Pr\,\Delta\tau}{(\Delta y^{*})^{2}}\right\}$$
$$-\left(\frac{UR+|UR|}{2\Delta x^{*}}\omega_{i,j+1}^{*0}-\left(\frac{UL+|UL|}{2\Delta x^{*}}\right)\omega_{i,j-1}^{*0}\right)*\frac{\Delta\tau}{2}-\left[\frac{VA-|VA|}{2\Delta y^{*}}\omega_{i+1,j}^{*0}-\left(\frac{VB+|VB|}{2\Delta y^{*}}\right)\omega_{i-1,j}^{*0}\right]*\frac{\Delta\tau}{2}$$
$$+Pr\left[\frac{\omega_{i,j+1}^{*0}+\omega_{i,j-1}^{*0}}{(\Delta x^{*})^{2}}\right]*\frac{\Delta\tau}{2}+Pr\left[\frac{\omega_{i+1,j}^{*0}+\omega_{i-1,j}^{*0}}{(\Delta y^{*})^{2}}\right]*\frac{\Delta\tau}{2}+Gr\,Pr^{2}\left(\frac{\theta^{0}_{PCM\ \ i,j+1}-\theta^{0}_{PCM\ \ i,j-1}}{2\Delta x^{*}}\right)*\frac{\Delta\tau}{2} \qquad (9)$$

where;

$$UR=\frac{u^{*}_{i,j+1}+u^{*}_{i,j}}{2},\ UL=\frac{u^{*}_{i,j-1}+u^{*}_{i,j}}{2},\ VA=\frac{v^{*}_{i+1,j}+v^{*}_{i,j}}{2}\ \text{and}\ VB=\frac{v^{*}_{i-1,j}+v^{*}_{i,j}}{2}$$

The finite difference representation for the stream function is,

$$\Psi^{*}_{i,j}=\{\frac{\Psi^{*}_{i,j+1}+\Psi^{*}_{i,j-1}}{(\Delta x^{*})^{2}}+\frac{\Psi^{*}_{i+1,j}+\Psi^{*}_{i-1,j}}{(\Delta y^{*})^{2}}-\omega^{*}_{i,j}\}/\{2/(\Delta x^{*})^{2}+2/(\Delta y^{*})^{2}\} \qquad (10)$$

Also, the liquid PCM velocities can be simply obtained by, $u^{*}=\frac{\Psi^{*}_{i+1,j}-\Psi^{*}_{i-1,j}}{2\Delta y^{*}}$

and $v^{*}=-\frac{\Psi^{*}_{i,j+1}-\Psi^{*}_{i,j-1}}{2\Delta x^{*}}$.

The energy equation for the liquid phase is formulated with the ADI technique that gives the solution in x direction at half time step and in y direction after complete time step as:

In x- direction:

$$\theta_{i,j-1}^{0+1/2}+\left\{-\left(\frac{\overset{0}{UL}+|\overset{0}{UL}|}{2\Delta x^{*}}\right)-\frac{1}{(\Delta x^{*})^{2}}\right\}+\theta_{i,j}^{0+1/2}\left\{\frac{2}{\Delta\tau}+\frac{\overset{0}{UR}+|\overset{0}{UR}|-\overset{0}{UL}+|\overset{0}{UL}|}{2\Delta x}+\frac{2}{(\Delta x)^{2}}\right\}$$
$$+\theta_{i,j+1}^{0+1/2}\left(\frac{\overset{0}{UR}-|\overset{0}{UR}|}{2\Delta x^{*}}-\frac{1}{(\Delta x^{*})^{2}}\right)=\theta_{i,j}^{0}\left\{\frac{2}{\Delta\tau}-\frac{\overset{0}{VA}+|\overset{0}{VA}|-\overset{0}{VB}+|\overset{0}{VB}|}{2\Delta y^{*}}-\frac{2}{(\Delta y^{*})^{2}}\right\} \qquad (11)$$
$$+\theta_{i+1,j}^{0}\left\{-\left(\frac{VA-|VA|}{2\Delta y^{*}}\right)+\frac{1}{(\Delta y^{*})^{2}}\right\}+\theta_{i-1,j}^{0}\left\{\left(\frac{VB+|VB|}{2\Delta y^{*}}\right)+\frac{1}{(\Delta y^{*})^{2}}\right\}$$

In y- direction:

$$\theta^{n}_{i-1,j}\left\{-\left(\frac{VB^{0+1/2}+|VB|^{0+1/2}}{2\Delta y^{*}}\right)-\frac{1}{(\Delta y^{*})^{2}}\right\}+\theta^{n}_{i,j}\left\{\frac{VA^{0+1/2}+|VA|^{0+1/2}-VB^{0+1/2}+|VB|^{0+1/2}}{2\Delta y^{*}}+\frac{2}{\Delta\tau}+\frac{2}{(\Delta x^{*})^{2}}\right\}$$
$$+\theta^{n}_{i+1,j}\left(\frac{VA^{0+1/2}-|VA|^{0+1/2}}{2\Delta y^{*}}-\frac{1}{(\Delta y^{*})^{2}}\right)=\theta^{0+1/2}_{i,j}\left\{\frac{2}{\Delta\tau}-\frac{UR^{0+1/2}+|UR|^{0+1/2}-UL^{0+1/2}+|UL|^{0+1/2}}{2(\Delta x^{*})^{2}}-\frac{2}{(\Delta x^{*})^{2}}\right\} \quad (12)$$
$$+\theta^{0+1/2}_{i,j+1}\left\{-\left(\frac{UR^{0+1/2}-|UR|^{0+1/2}}{2\Delta x^{*}}\right)-\frac{1}{(\Delta x^{*})^{2}}\right\}+\theta^{0+1/2}_{i,j-1}\left\{\left(\frac{UL^{0+1/2}+|UL|^{0+1/2}}{2\Delta x^{*}}\right)-\frac{1}{(\Delta x^{*})^{2}}\right\}$$

b- for the modified conduction model

The PCM energy equation, Eq.(5), is approximated in a difference form to be solved using the ADI technique utilizing the grid notation shown in Fig.(2) as:

In x- direction:

$$\theta^{0+1/2}_{i,j+1}\left(\frac{-\alpha_r}{(\Delta x^{*})^{2}}\right)+\theta^{0+1/2}_{i,j}\left(\frac{2\alpha_r}{(\Delta x^{*})^{2}}+\frac{2}{\Delta\tau}\right)+\theta^{0+1/2}_{i,j-1}\left(\frac{-\alpha_r}{(\Delta x^{*})^{2}}\right)=\theta^{0}_{i,j}\left(\frac{2}{\Delta\tau}-\frac{2\alpha_r}{(\Delta y^{*})^{2}}\right)+\frac{\alpha_r(\theta^{0}_{i+1,j}+\theta^{0}_{i-1,j})}{(\Delta y^{*})^{2}} \quad (13)$$

In y- direction:

$$\theta^{n}_{i-1,j}\left(\frac{-\alpha_r}{(\Delta y^{*})^{2}}\right)+\theta^{n}_{i,j}\left(\frac{2}{\Delta\tau}+\frac{2\alpha_r}{(\Delta y^{*})^{2}}\right)+\theta^{n}_{i+1,j}\left(\frac{-\alpha_r}{(\Delta y^{*})^{2}}\right)=\theta^{0+1/2}_{i,j}\left(\frac{2}{\Delta\tau}-\frac{2\alpha_r}{(\Delta x^{*})^{2}}\right)+\frac{\alpha_r(\theta^{0+1/2}_{i,j+1}+\theta^{0+1/2}_{i,j-1})}{(\Delta x^{*})^{2}} \quad (14)$$

c) for enhanced finned channels model

The energy equations of the PCM, working fluid and the fins are approximated in difference forms with the aid of the grid notation shown in Fig.(2) as follows:

i-for the PCM

$$\theta^{n}_{i,j}=\theta^{0}_{i,j}\left(1-\frac{2\alpha_r\Delta\tau}{(\Delta x^{*})^{2}}-\frac{2\alpha_r\Delta\tau}{(\Delta y^{*})^{2}}\right)+\frac{\alpha_r\Delta\tau}{(\Delta x^{*})^{2}}(\theta^{0}_{i+1,j}+\theta^{0}_{i-1,j})+\frac{\alpha_r\Delta\tau}{(\Delta y^{*})^{2}}(\theta^{0}_{i,j+1}+\theta^{0}_{i,j-1}) \quad (15)$$

ii - for the working fluid

$$\frac{\beta_1\Delta\tau}{2\Delta x^*}\theta^n_{i+1}+(1+\beta_2\Delta\tau)\theta^n_i-\frac{\beta_1\Delta\tau}{2\Delta x^*}\theta^n_{i-1}=\theta^0_i+\beta_2\Delta\tau\theta^0_{PCM} \tag{16}$$

where, $\beta_1=\mathrm{Re}\frac{H}{D_H}\frac{\nu_f}{\alpha_l}$ and $\beta_2=2\mathrm{Nu}\frac{H^2}{D_H w}\frac{\alpha_f}{\alpha_l}$

iii- for the fins

$$\frac{-\beta_3\Delta\tau\theta^n_{j+1,fin}}{(\Delta y^*)^2}+\left(1+\frac{2\beta_3\Delta\tau}{(\Delta y^*)^2}+\frac{2\beta_4\Delta\tau}{(\Delta x^*)^2}\right)\theta^n_{j,fin}-\frac{\beta_3\Delta\tau\theta^n_{j-1,fin}}{(\Delta y^*)^2}=\theta^0_{j,fin}+\frac{\beta_4\Delta\tau(\theta^0_{PCM,i+1,j}+\theta^0_{PCM,i-1,j})}{\Delta x^*} \tag{17}$$

where, $\beta_3=\frac{\alpha_{fin}}{\alpha_l}$ and $\beta_4=\frac{K_{PCM}}{K_{fin}}\frac{H}{z}\frac{\alpha_{fin}}{\alpha_l}$

4. STABILITY OF THE COMPUTATIONAL PROCEDURE

The time steps are adopted such that the conditions of the stability and convergence of the numerical solution are satisfied for each model and the following time steps are found:

4.1. Natural convection model

i) for the vorticity equation, Eq.(9),

$$\Delta\tau\le\frac{2}{\frac{UR+|UR|-UL+|UL|}{2\Delta x^*}+\frac{VA+|VA|-VB+|VB|}{2\Delta y^*}+2\mathrm{Pr}\left(\frac{1}{(\Delta x^*)^2}+\frac{1}{(\Delta y^*)^2}\right)} \tag{18}$$

ii) for the energy equation in x-direction, Eq(11),

$$\Delta\tau\le\frac{2}{\frac{VA+|VA|-VB+|VB|}{2\Delta y^*}+\frac{2}{(\Delta y^*)^2}} \tag{19}$$

iii) for the energy equation in y-direction, Eq(12),

$$\Delta\tau\le\frac{2}{\frac{UR+|UR|-UL+|UL|}{2\Delta x^*}+\frac{2}{(\Delta x^*)^2}} \tag{20}$$

4.2. Modified conduction model

The time steps for the energy equation of the PCM in x and y directions Eqs.(13,14) are $\Delta t\le 1\Big/\frac{2\alpha_r}{(\Delta y)^2}$ and $\Delta t\le 1\Big/\frac{2\alpha_r}{(\Delta x^*)^2}$, respectively.

4.3. Enhanced finned channels model

The time step as obtained from the energy equation of the PCM, Eq.(15) is; $\Delta t \le 1 \Big/ \left(\frac{2\alpha_r}{(\Delta x)^2} + \frac{2\alpha_r}{(\Delta y)^2} \right)$. Because of the implicit nature of the energy equations for both the working fluid and the fins, the solution is unconditionally stable.

4.4. Computational Procedure

At early melting time, the natural convection effect is not appeared. Therefore, the simple conduction energy equation of the PCM is solved using the ADI technique. The solution using ADI is performed firstly in x-direction at the half of the time step$\left(\tau + \frac{\Delta\tau}{2}\right)$. After that, the solution is obtained at the end of the time step$(\tau + \Delta\tau)$. Therefore for each row or column, the set of equations in the scheme forms a tri-diagonal matrix which can be solved using Thomas algorithm [25]. The natural convection effect is considered as the melted layer is of order 4 mm thickness as described by Sakr [2]. At this time, the program begins to solve the vorticity equation Eq.(9). After that the stream function for all internal nodes in the liquid phase is calculated from Eq.(10) using Gauss-Seidel iterative method. Many iterations are performed until reaching the prescribed accuracy at each node in the domain such that $\left|\frac{\Psi^k - \Psi^{k-1}}{\Psi^k}\right| \le 10^{-3}$, where k is the iteration level. The program begins to compute the velocity distributions which are substituted in the energy equation of the liquid phase of the PCM. As the temperature distribution of the PCM is obtained, the melted volume ratio and the amount of the heat stored can be calculated. Then, the program begins to solve the energy equation Eq.(13) and Eq.(14)] in modified conduction model considering the effective (enhanced) thermal conductivity of the melted liquid The effective thermal conductivity of the melted PCM is related to the dimensionless time, Rayleigh number, Stefen number, subcooled number, and aspect ratio as $\left(\frac{K_{eff}}{K_l} = a\, Ra^b\, \tau^c\, ste^d\, Sc^e\, AR^f\right)$. The constants a, b, c, d, e, and f are changed in the numerical solution until an acceptable agreement between the predictions of the natural convection and the modified conduction models for the melted volume ratio and the amount of the heat stored. A parametric study is performed for different initial condition (Subcooled number) and heating condition (Rayleigh and Stefen numbers) at different aspect ratios to get the correlation of the effective thermal conductivity of the melted PCM. This correlation is utilized in the enhanced finned channels model with PCM packed in the space between the flow channels (single or multi pass flow configurations) to simplify the solution. In this part of the study, the energy equation of the PCM, Eq.(15), the working fluid, Eq.(16), and the

fins, Eq.(17), are solved to obtain the temperature distribution in the PCM, the working fluid and the fins, respectively.
The set of the equations for the nodes of the fluid and the fins are written in the form of the tri-diagonal matrix which can be solved using Thomas algorithm. The computations are performed on personal computer using a FORTRAN program.

5. EXPERIMENTAL INVESTIGATION

The objective of the present experimental work is to validate the present numerical modeling predictions. For this purpose, an experimental apparatus was designed, fabricated, and constructed. A schematic diagram of the present experimental setup is presented in Fig.(2). It comprises the test section, hot water circulation circuit and instrumentation.

5.1 The Test Section

The test section is composed of plexiglass container, the phase change material (storage medium), the finned flow channels and the guard heater. Figure (4) shows the details of the test section. The internal dimensions of the storage container are 480 mm length, 250 mm height, 130 mm width and 8 mm wall thickness. The inlet flow distributor is equipped by a partition to achieve two pass flow configuration as shown in Fig.(4b). The hot water passes through two aluminum channels of thickness 1.5 mm and internal dimensions of 480 mm length, 250 mm height and 10 mm width. The flow channels are spaced by 65 mm. Aluminum fins of thickness 1.25 mm and 20mm height are installed on the flow channels at a pitch either equals 60 mm or 96 mm. The PCM used in the present experimental work is a paraffin wax which has nearly melting point of 53°C. The themophysical properties of the paraffin wax used in the present experimental work are obtained from [2]. The paraffin wax is melted and poured in the storage container around the flow channels such that the PCM height is 220 mm and the gap above the PCM surface is accounted for the expansion of the PCM during the melting process. A Nickel-Chromium guard heater, fabricated from electric resistance strips 5 mm wide, 0.25 mm thick and 1.2 Ω/m turned around a mica sheet 1 mm thickness and sandwiched between another two mica sheets, is connected to a voltage regulator (500 W) and placed at the top surface of the storage container to minimize the heat loss from the expanded PCM during the melting process. The power supplied to the guard heater is regulated to maintain the average temperature of air inside the gap above the PCM surface at the PCM melting temperature (53 °C ± 2 °C).

5.2 The Hot Water Circulation Loop

A closed pumping loop system utilizing water as the working fluid was used to supply the test section with constant temperature hot water. A water tank of 340 mm diameter and 800 mm height is fabricated from galvanized steel sheet 1

mm thickness and mounted on a steel base at the laboratory floor. The water is primary heated by two electric heaters (1200 W/heater) with thermostats. Another heater of 600 W is connected to thermostatic temperature controller placed at the pump suction. A centrifugal pump (0.75 hp) with stainless steel impeller is used to circulate the hot water through the test loop.

5.3 Measurements and Instrumentation

Teflon-insulated copper-constantan thermocouples of 0.5 mm diameter are used to measure the temperature distribution inside the PCM and the hot water flow inlet and outlet temperatures. The readings of the thermocouples are directly indicated using a digital thermometer which is able to read the temperature to one-tenth degree. The used digital thermometer and the thermocouples are calibrated prior installing in the test section. The hot water mass flow rate is measured using a calibrated orifice meter. Also, a multimeter is used to measure the electric resistances and the voltage drop across the heaters.

6. RESULTS AND DISCUSSION

The isotherms and stream functions, melted volume ratio and the amount of the heat stored during melting process were predicted by applying the natural convection analysis to the physical model shown in Fig.(1-a). Preliminary runs were carried out to validate the present predictions of the natural convection model. The results of the predicted melted volume ratios were compared with previous experimental data of [26, 2] and good agreements were found as shown in Fig.(3). In fact, one of the main objectives of the present study is to detect an effective thermal conductivity (K_{eff}) for the melted PCM. This was accomplished by comparing the predictions of a modified conduction model based on the concept of K_{eff} with that of the natural convection model for the physical model shown in Fig.(1-a). The present numerical analysis was adapted to obtain a correlation for the K_{eff} as a function of the different investigated parameters. The influences of Raleigh number, Stefen number, Subcooled number, dimensionless time and the aspect ratio on K_{eff} were investigated and the following correlation was obtained:

$$\frac{K_{eff}}{K_l} = 0.225 Ra^{0.225} \tau^{0.5} ste^{0.25} Sc^{-0.15} AR^{0.5} \qquad (21)$$

Figure (4) illustrates a comparison between the predictions of both the natural convection (N.C.) model and the modified conduction (M.C.) model, based on the correlated K_{eff}, for the storage system shown in Fig.(1-a) at different aspect ratios (AR). Generally good agreement was found between the predictions of the two models within the investigated range of the aspect ratio. This in fact confirms that the obtained correlation for K_{eff}, Eq.(21), is applicable and it can simulate the effect of the natural convection current.

Therefore, the modified conduction model was adapted to predict the thermal performance of an enhanced storage system shown in Fig.(1-b) utilizing the correlation of the (K_{eff}), Eq.(21). The temporal temperature distributions of the PCM in the space between two successive flow-channels for a storage unit with plain channels were predicted and experimentally measured at different operating conditions. The results at ($Ra=3.7x10^9$, Ste=0.14 and Sc=0.29) for two different Reynolds numbers (Re_{DH}=356 and 684) are shown in Fig.(5). Generally, fair agreement was noticed between the present predictions and the experimental data as shown in Fig.(5). This in fact is a further confirmation of the validity of the present predictions. The variation of the melted volume ratio with the time for a unit with plain flow-channels is shown in Fig.(6) for Sc=0.29 at three different Reynolds numbers. It was found that the melted volume ratio is mainly dependent on the fluid inlet temperature which is represented by Rayleigh number. This is due to the increase in the rate of heat exchange and the enhancement in natural convection currents as a result of increasing the fluid inlet temperature. The discrepancy between the numerical and experimental results becomes noticeable with the increase in the melted volume due to the extremely high natural convection effect. Figure (7) shows the effect of Reynolds number on the melted volume ratio at different operating conditions. It was found that beyond a value of Re_{DH} of about 300, the thermal resistance of the fluid side becomes very small such that the heat transfer rate is driven only by the thermal resistance of the PCM side. Therefore, Reynolds number, beyond a value of 300, becomes ineffective on the storage performance as shown in Fig.(7). The effect of the flow-channel pitch (p) on the storage performance of plain-channels storage units with the same storage volume operate at the same fluid mass flow rate is illustrated in Fig.(8). It was found that the storage performance is strongly enhanced with the decrease in the channel pitch. This is simply due to the increase in the heat transfer area regardless of the decrease in Re_{DH} which is already ineffective.

The enhancement in the storage characteristics using units with externally finned flow-channels (fins were affixed on the PCM side) was extensively investigated herein the present work. Figure (9) shows the effect of the use of finned channels on the melted volume ratio at different operating conditions. Generally, fins are made of metals with higher thermal conductivities. Thus, when fins penetrate and break the PCM which has a lower thermal conductivity they elevate the diffusion behavior in the PCM. Therefore, the presence of fins in the PCM side enhances the overall heat transfer coefficient in general and in accordance enhances the performance of the storage. Figure (10) shows that the enhancement effect of the finned channels becomes significant with time. This is due to the propagation of natural convection currents as the volume of melted liquid increases. The effects of the fin pitch and length on the thermal storage characteristics of a unit with finned channels are illustrated in Fig.(11) and Fig.(12), respectively. It was found that both the increase in fin concentration

(the decrease in the fin pitch) and the increase in the fin length enhance the storage performance in general. These enhancements are due the excessive reduction in the thermal resistance of the PCM side as a result of the increase in the heat transfer area. The effect of the fin thickness was also investigated and it was found that the storage enhancement is independent of fin thickness. This is because of the higher thermal conductivity of the fin material, compared with that of the PCM, it conducts heat with almost negligible temperature gradient and it does not need for further cross-sectional area (additional thickness) to enhance the heat transfer.

Moreover, the present experimental data in addition to the present extended predictions were utilized to correlate the performance characteristics of the enhanced latent heat storage systems. The following correlations were obtained for the melted volume ratio and the heat stored as functions of Rayleigh number, time, subcooled number, Reynolds number, the pitch and the length of fins and the channel pitch:

i) The melted volume ratio;

$$\frac{V}{V_o} = 1.34 \times 10^{-5} Ra^{0.67} \tau^{0.58} Sc^{-0.03} Re_{DH}^{0.11} \left(\frac{S}{H}\right)^{-0.07} \left(\frac{\ell}{H}\right)^{0.11} \left(\frac{p}{H}\right)^{-0.19} \quad (22)$$

ii) The amount of the heat stored;

$$\frac{Q}{m_{PCM}.h_{sf}} = 7.27 \times 10^{-6} Ra^{0.61} \tau^{0.63} Sc^{0.07} Re_{DH}^{0.11} \left(\frac{S}{H}\right)^{-0.07} \left(\frac{\ell}{H}\right)^{0.10} \left(\frac{p}{H}\right)^{-0.06} \quad (23)$$

The correlated values were plotted versus the predicted values as shown in Fig.(13) and it was found that most of the data points are in fair agreement with maximum deviations of $\pm 20\%$. Therefore, the present correlations are valid within the following ranges of the different parameters as: $(10^6 \le Ra \le 10^{11})$, $(0.01 \le Sc \le 0.38)$, $Re_{Dh} \le 1636$, $(0.1176 \le S/H \le 0.889)$, $(0.02 \le \ell/H \le 0.1)$ and $(3 \le p/H \le 16)$ with maximum deviations of $\pm 20\%$.

7. CONCLUSIONS

On view of the present results the following conclusions were drawn:

1- The effective thermal conductivity of the melted PCM was correlated as a function of Rayleigh, Stefen and Subcooled numbers, aspect ratio and the dimensionless time.

2- The modified conduction model based on the concept of the effective thermal conductivity of the melted PCM is a powerful technique in predicting the performance of the latent heat storage systems with different configurations.

3- Reynolds number is critically affect performance of storage systems with fluid flow channels as beyond to a value of 300 Reynolds number becomes ineffective.

4- The decrease in the flow channel pitch enhances the performance of the plain channel storage systems in general.

5-The enhancement in the storage characteristics of the finned channel systems with PCM is strongly dependent on the fin pitch and the fin length while it does not depend on the fin thickness.

6- New correlations were obtained for the melted volume ratio and the stored heat in finned channel latent heat storage systems within the investigated ranges of the different parameters.

NOMENCLATURE

SI system of unit is used for the whole parameters within the present study.

c	specific heat
D_H	hydraulic diameter
H	storage volume height
h_{sf}	latent heat of the PCM
K	thermal conductivity
L	pass length
ℓ, l	fin height
n	normal vector on the surface
p	flow channel pitch
Q	heat stored
s	fin pitch
T	temperature
t	time, fin thickness
U	overall heat transfer coefficient
u	velocity in x-direction
V	PCM melted volume
Vo	initial PCM volume
v	velocity in y-direction
w	width of the storage volume
x	distance in x-direction
y	distance in y-direction

Greek Letters

α	thermal diffusivity
β	thermal expansion of PCM
$\beta_{1,2,3,4}$	coefficients in Eqs.(16,17)
Δ	difference operator
ν	kinematic viscosity
θ	dimensionless temperature
ρ	density
τ	dimensionless time, $\tau=\alpha t/H^2$
ω	vortocity
ψ	stream function

Subscripts

c	channel
DH	hydraulic diameter
eff	effective property of the liquid PCM
f	working fluid
fluid, o	outlet of the working fluid
fin	fin property
in	inlet
i, j	grid notation
l	liquid phase in the PCM
left	left side
m	mushy phase in the PCM
mp	melting point
o	reference value
overall	overall property
PCM	phase change m aterial
r	relative
ref	reference
right	right side
s	solid phase in the PCM
sf	solid to liquid transformation
w	adjacent wall

Superscripts

*	dimensionless
0	old time
o+1/2	at the half of the time step
n	at the end of the time step
k	iteration level

Abbreviations

M.C.	modified conduction
N.C.	natural convection
PCM	phase change material

Dimensionless Groups

Gr Grashof number, $Gr = g\beta(T_{ref} - T_{mp})H^3/\nu^2$

Nu Nusselt number, $Nu = U_{overall} D_H / K_f$

Pr Prandtl number, $Pr = \nu_l / \alpha_l$

Ra Rayleigh numbe, Ra=Gr*Pr

Re Reynolds number, $Re = V_f D_H / \nu_f$

Sc subcooled number, $Sc = c_s(T_{mp} - T_{initial})/h_{sf}$

Ste Stefen number, $Ste = c_l(T_{ref} - T_{mp})/h_{sf}$

REFERENCES

1- Ilken, B. Z. and Toksoy, M., "The Solution Methods Used in the Heat Transfer problems With Phase Change", Research Paper, Dokuz Eylul University, Izmir, Turkey, No. FBE/MAK-89-AR-131, 1989.

2- Sakr R.,"Melting Heat Transfer In Rectangular Enclosures-An Experimental and Numerical Study", Ph. D. Thesis, Faculty of Eng., Cairo Univ., 1994.

3- Micho Yanadori, and Takashi Mosuda, "Heat Transfer study on a Heat Storage Container With a Phase Change Material (Part 2: Heat Transfer in the Melting Process in a Cylindrical Heat Storage Container", Solar Energy, Vol. 42, No.1, pp. 27-34, 1989.

4- Zhen-Xiang Gong and Arun S. Mujumdor, "Finite Element Analysis of Cyclic Heat Transfer in a Shell and Tube Latent Heat Energy Storage Exchanger", Applied Thermal Engineering, Vol.17, No.6, pp.583-591, 1997

5- Rousseau, P.B. and Lacroix, M., "Study of The Thermal Performance of a Multi Layers PCM Storage Unit", Energy Conv., Vol.37, pp.599-609, 1996.

6- Marshal R. and Dietsch, C., "Comparison of Paraffin Wax Storage Subsystem Models Using Liquid Heat Transfer Media", Solar Energy, Vol. 29 No. 6, pp. 503-511, 1982.

7- Hasan, A., "Phase Change Material Energy Storage System Employing Palmitic Acid", Solar Energy, Vol. 52, No. 2, pp. 143-154, 1994.

8- Esen, M., Durmus, A. and Durmus, A., "Geometric Design of Solar-Aided Latent Heat Store Depending on Various Parameters and Phase Change Materials", Solar Energy, Vol. 62, No. 1, pp. 19-28, 1998.

9- Eman-Bellah, S. M., Assassa, G. R., "Enhancing the Thermal Conductivity of Latent Heat Storage System", Proc. of the 7th Int. Conf. On Energy and Environment, pp. 331-340, Cairo, Egypt, 2000.

10- Hoogendoorn, C.J. and Bart G.C., "Performance and Modeling of Latent Heat Stores", Solar Energy, Vol. 48, No.6, pp. 53-58, 1992.

11- Abdel-Moneim, S.A., Atwan, E.F. and Sakr, R.Y., "Numerical Study of Packed Bed Thermal Energy Storage Systems with Encapsulated Phase Change Material", Engng. Res. Jour. Helwan Univ., Faculty of Eng., Matria, Cairo, Vol. 58, pp. 77-92, August 1998.

12- Beasly D.E. and Ramanaroyanon C.,"Thermal Response of a Packed Bed of Spheres Containing a Phase Change Material", Int. J. of Energy Research, Vol. 12, pp. 253-265, 1989.

13- Jianfeng, W., Yingxiu, O. and Guangming, C., "Experimental Study on Charging Processes of A Cylindrical Heat Storage Employing Capsulated Multiple Phase Change Material", Energy Res.J., Vol.25, pp.439-447, 2001.
14- Hawlader, M.N., Udin, M.S. and Zhu, H.J. "Encapsulated Phase Change Material for Thermal Energy Storage: Experimental and Simulation", Energy Res. J., Vol.26, pp.159-171, 2002.
15- Velraj, R., Seeniraj, R.V., Hafner, B., Faber, C. and Schwarzer, K., "Heat Transfer Enhancement in a Latent Heat Storage System", Solar Energy, Vol. 65, No. 3, pp. 171-180, 1999.
16- Sparrow, E.M., Larsen E.D. and Ramsey J.W., "Freezing on a Finned Tube for either Conduction-Controlled or Natural-Convection-Controlled Heat Transfer", Int. J. Heat Mass Transfer, Vol. 24, pp. 273-284, 1981.
17- Padmanabhan, P.V. and Krishna Murthy M.V., "Outward Phase Change in a Cylindrical Annulus with Axial Fins on the Inner Tube", Int. J. Heat Mass Transfer, Vol. 29, pp. 1855-1866, 1986.
18- Eftekhar, J., Sheikh, A.H. and Lou, D.Y., "Heat Transfer Enhancement in a Paraffin Wax Thermal Storage System", J. Solar Energy Eng., Vol. 106, pp. 299-306, 1984.
19- Smith, R.N. and Koch, J.D., "Numerical Solution for Freezing Adjacent to a Finned Surface", Proc. of the 7th Int. Heat Transfer Conf., Munch, Germany, pp. 69-74, 1982.
20- Lacroix, M., "Study of the Heat Transfer Behavior of a Latent Heat Thermal Energy Unit with a Finned Tube", Int. J. Heat Mass Transfer, Vol. 36, pp. 2083-2092, 1993.
21- Yimer, B. and Adami, M., "Parametric Study of Phase Change Thermal Energy Storage Systems for Space Applications", Energy Conversion and Management, Vol. 38, No. 3, pp. 253-262, 1997.
22- Velraj, R., Seeniraj, R.V., Hafner, B., Faber, C. and Schwarzer, K., "Experimental Analysis and Numerical Modeling of Inward Solidification on a Finned Vertical Tube for Latent Heat Storage Unit", Solar Energy, Vol. 60, No. 5, pp. 281-290, 1997.
23- Costa M., Buddhi D. and Oliva A. "Numerical Simulation of a Latent Heat Thermal Energy Storage System with enhancement Heat Conduction" Energy Conversion Mgmt., Vol. 39, pp. 319-330, 1998.
24- Cao Y. and Faghri A., "A Numerical Analysis of Phase Change Problems Including Natural Convection" Transactions of ASME, Vol. 112, pp. 812-816, August 1990.
25- Kublbeck, K., Merker G.P. and Straub, "Advanced Numerical Computation of Two-Dimensional Time-Dependent Free Convection in Cavities", Int. J. Heat Mass Transfer, Vol. 23, pp. 203-217, 1980.
26- HO, C.J. and Viskanta, R., "Heat Transfer during Melting from An Isothermal Vertical Wall", Transactions of ASME, Vol.106, pp.12-19, 1984.

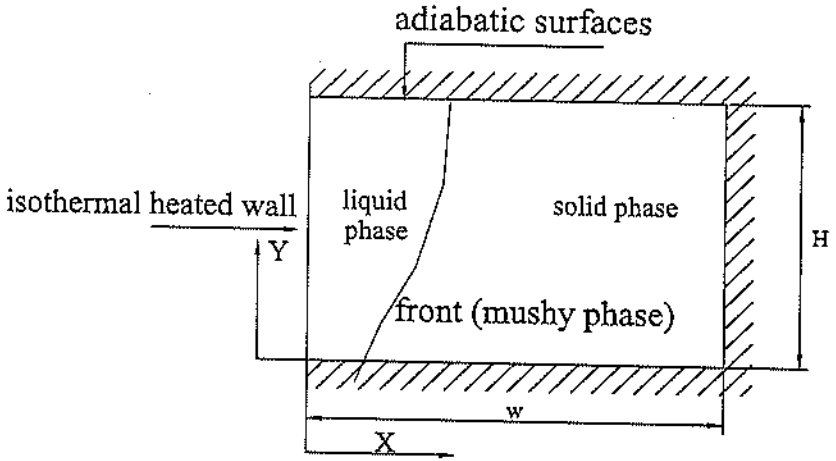

Physical model and boundary conditions

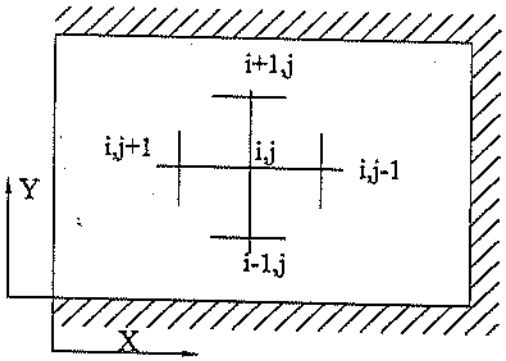

Grid notation

a) Natural convection and modified conduction models

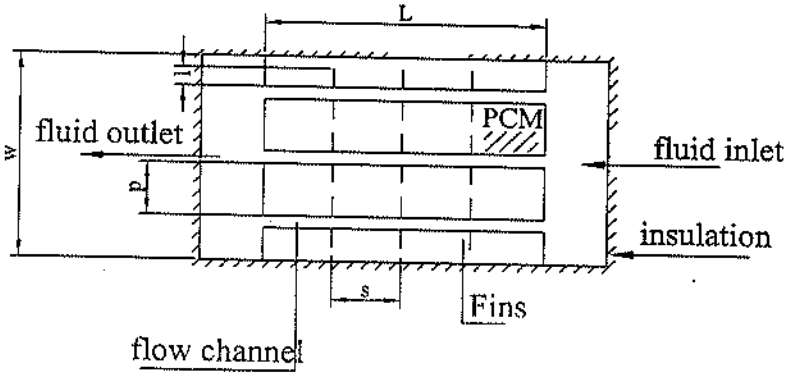

Physical model

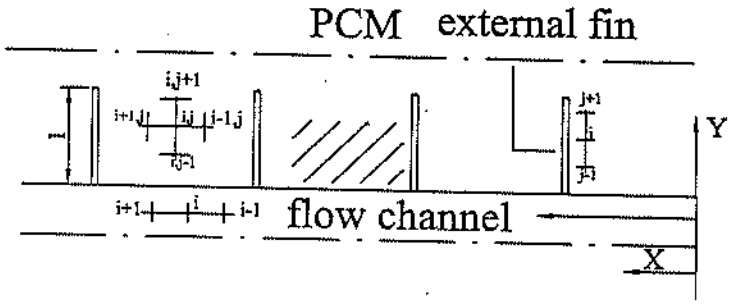

Solution domain and grid notation (repeated cell)

b) Enhanced finned channel model

Fig. (1): Physical models, boundary conditions and grid notations

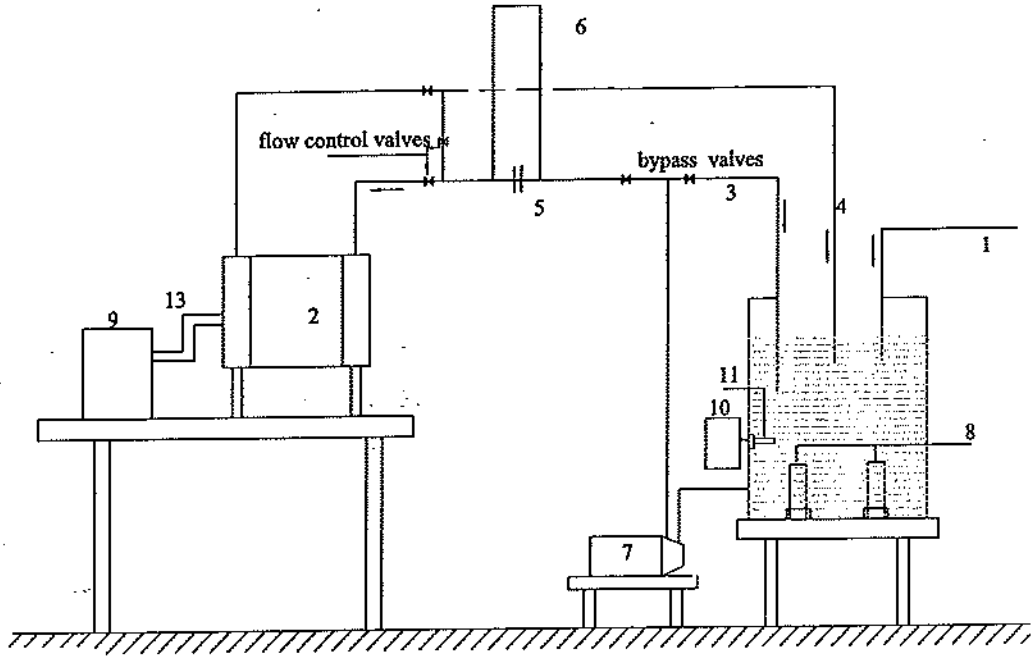

1-water supply
2-test section
3-by pass flow line
4-retun pass
5-orifice meter
6-inverted U-tube manometer
7- recirculation pump
8-two similar electric heaters (1200 kw)
9- Digital thermometer
10- temperature controller
11-electric heater(600 w)
13-thermocouples leadings

a) Schematic diagram of the test rig

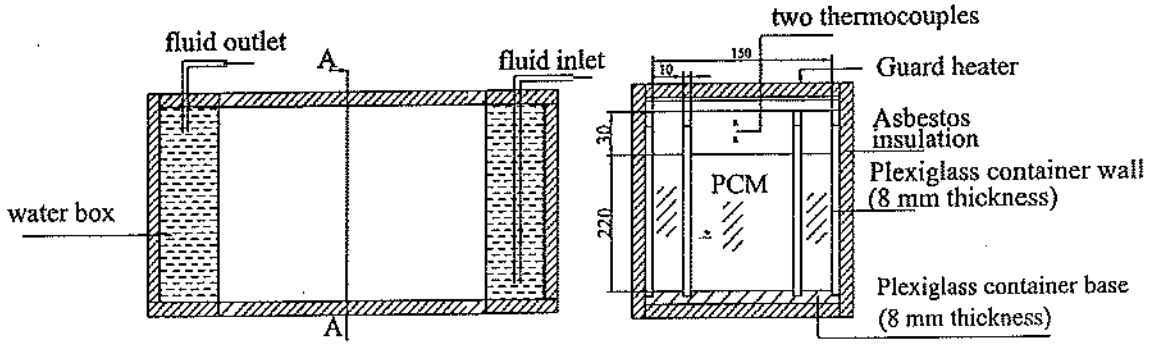

Sectional Elevation

sectional Side View at A-A

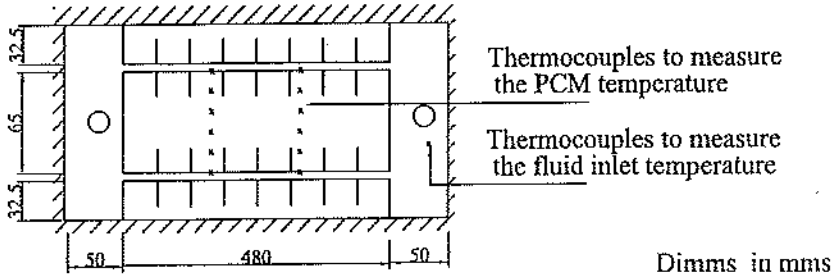

Dimms in mms

Plan

b) Details of the test section

Fig.(2): The experimental apparatus

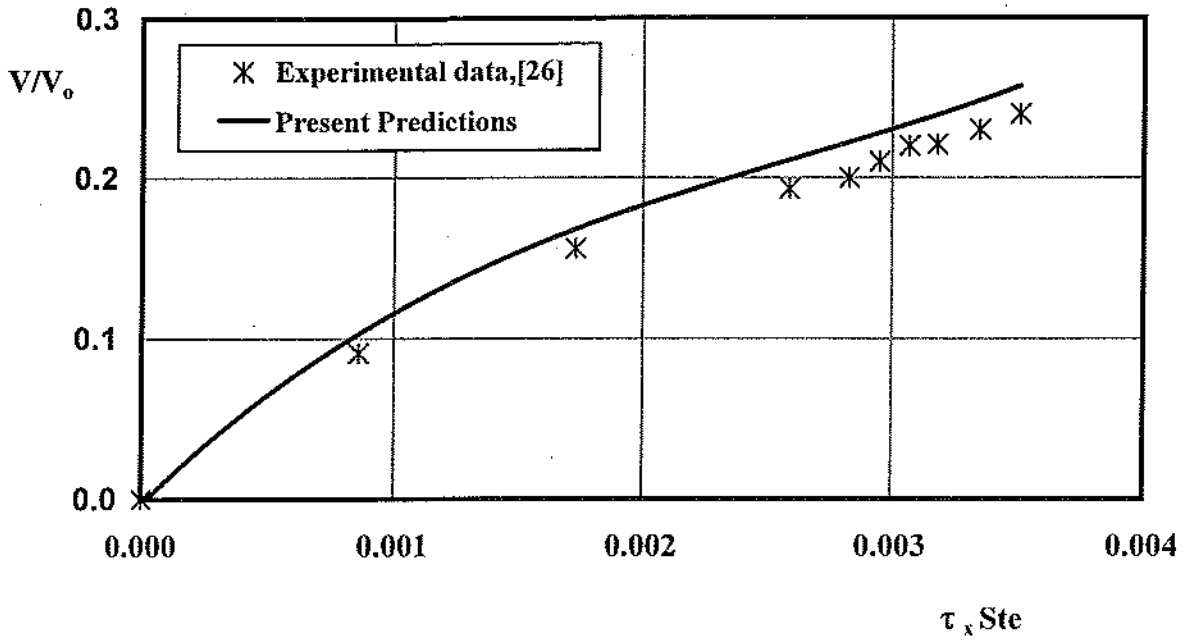

a) AR=2.63, Ra=6.3x10^7, Ste=0.063 and Sc=0.01

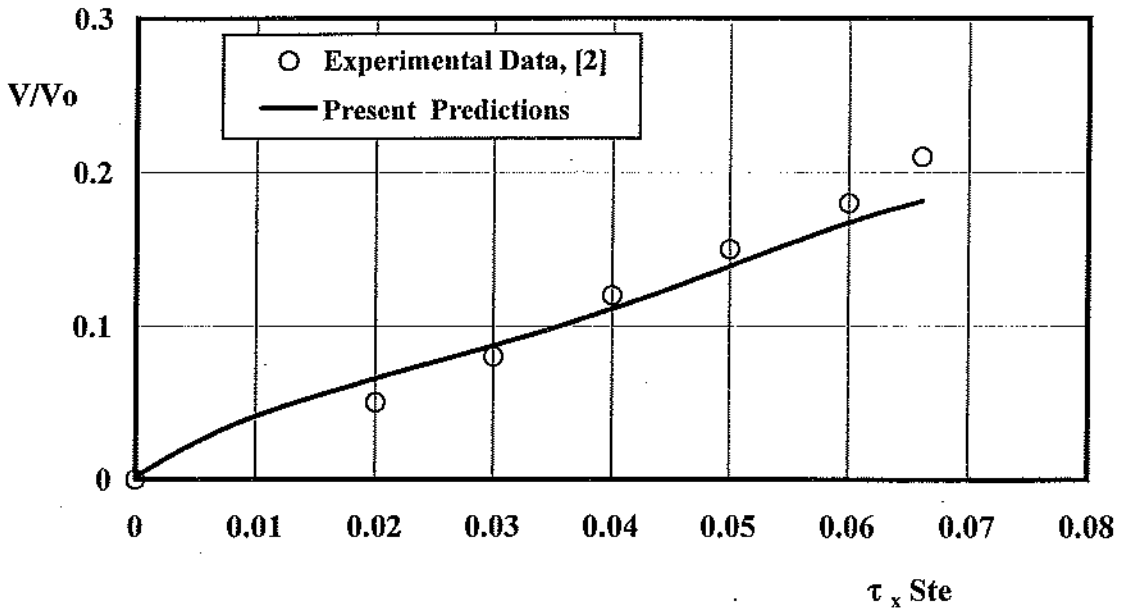

b) AR=0.38, Ra=2.0x10^7 , Ste=0.155 and Sc=0.27

Fig.(3): Validation of the present natural convection model: Compariosn of the predicted melted volume ratio with preveious experimental data.

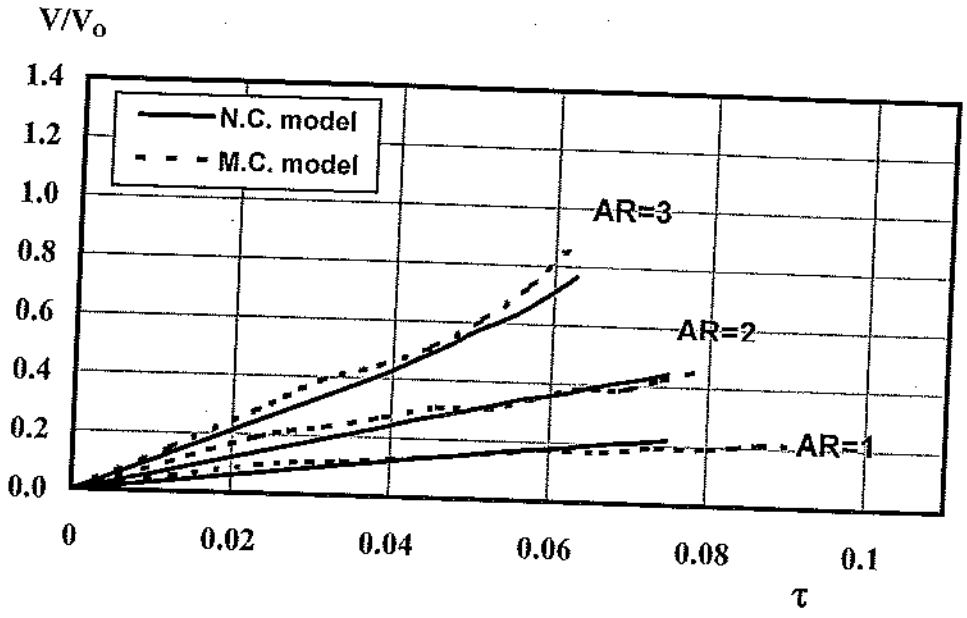

a) Temporal melted volume ratio at different aspect ratios

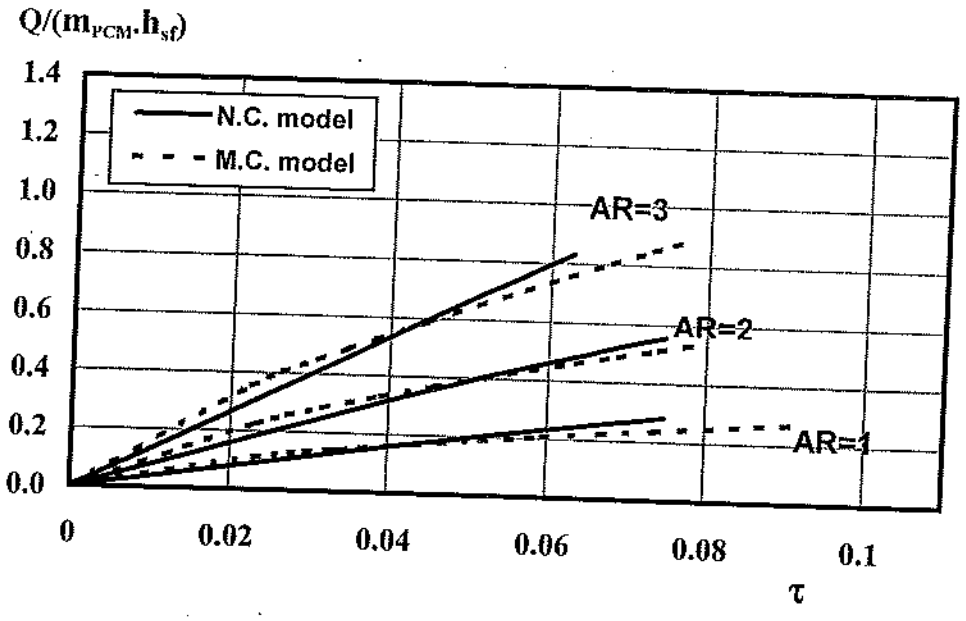

b) Temporal heat storage at different aspect ratios

Fig.(4): Validation of the present modified conduction model: Comparison with the natural convection model ($Ra=2.0x10^7$, Ste=0.155 and Sc=0.27)

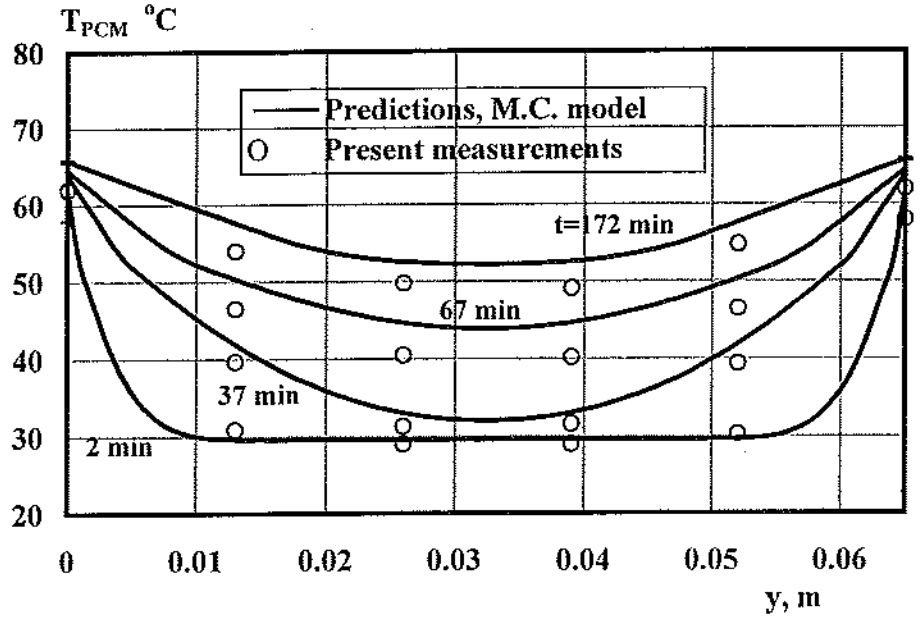

a) $Re_{DH} = 356$

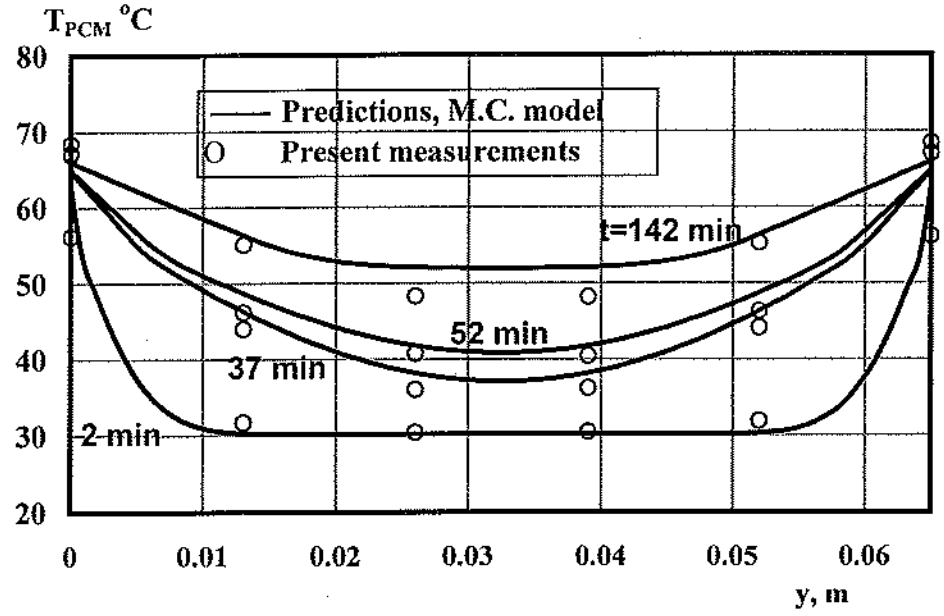

b) $Re_{DH} = 684$

Fig.(5): Temporal temperature distributions of the PCM for a storage unit with plain flow channels at different Reynolds number, ($Ra=3.76x10^9$, Ste=0.14 and Sc=0.29)

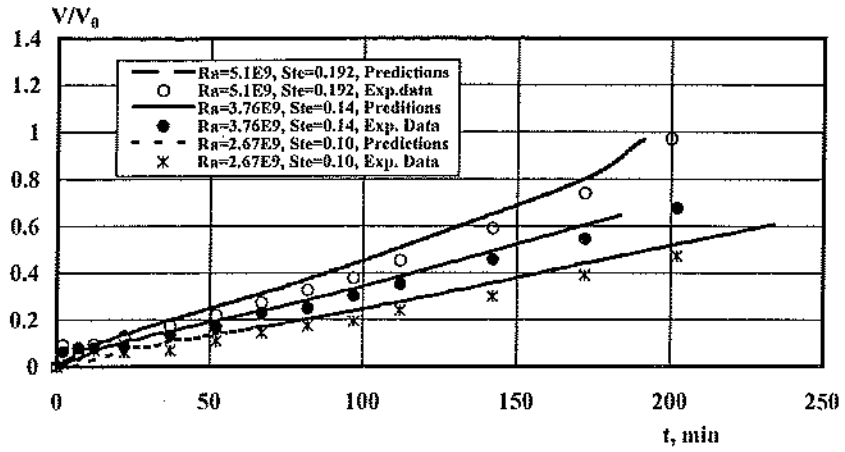

a) $Re_{DH} = 356$

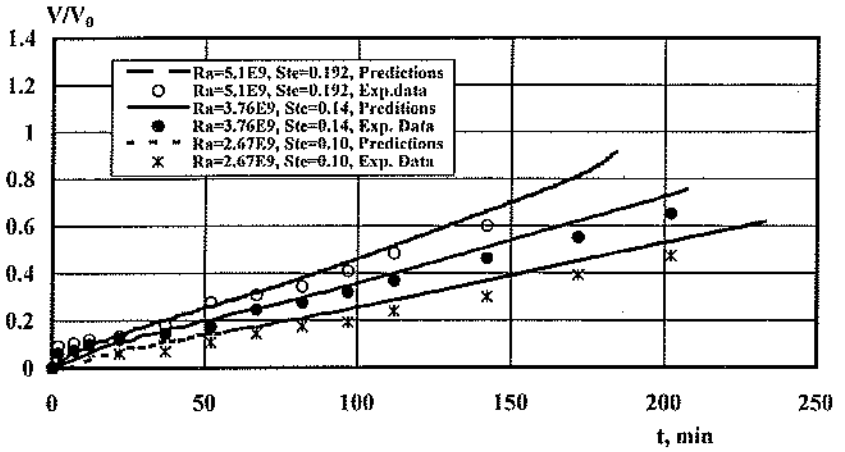

b) $Re_{DH} = 515$

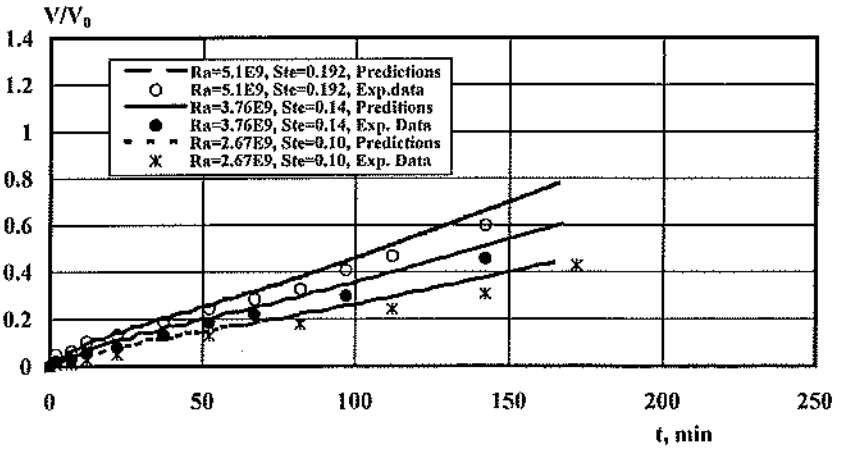

c) $Re_{DH} = 684$

Fig.(6): Temporal melted volume ratio for a storage unit with plain flow channels at different Reynolds numbers, Sc=0.29

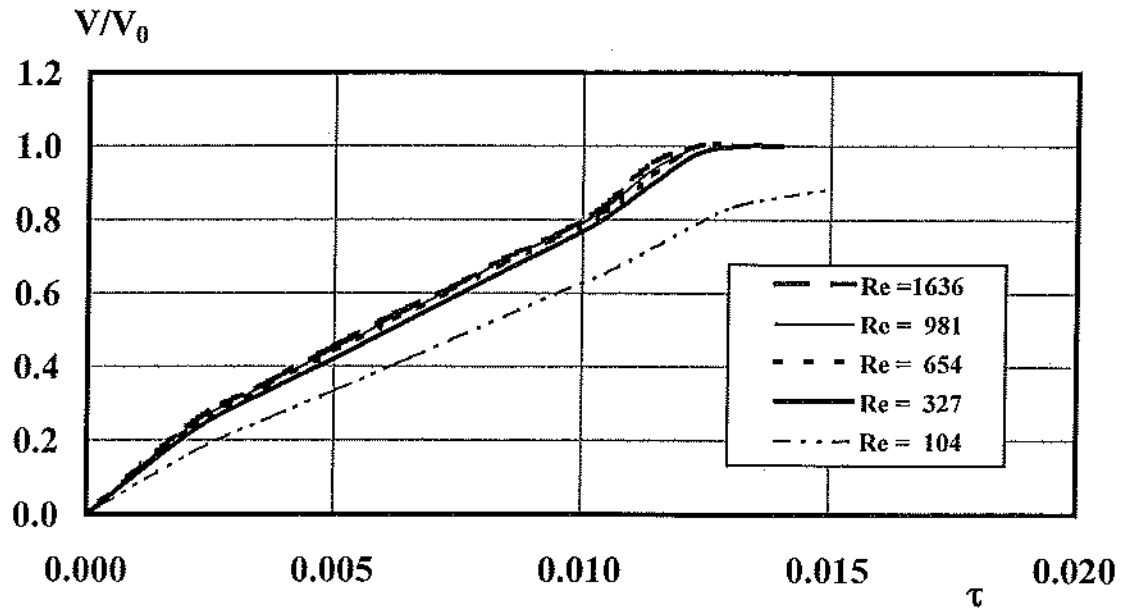

a) Melted volume ratio, ($Ra=9.6x10^9$, Ste=0.246 and Sc=0.18)

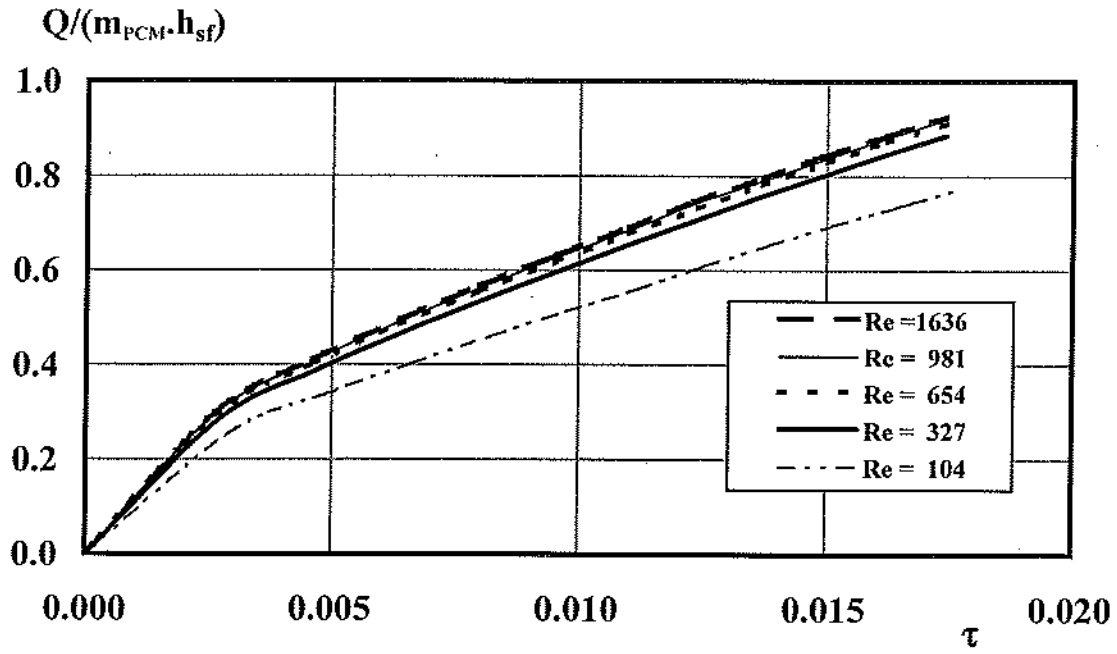

b) Heat storage, ($Ra=3.6x10^9$, Ste=0.091 and Sc=0.18)

Fig.(7): Transient performance of a storage unit with plain flow-channels at different Reynolds numbers

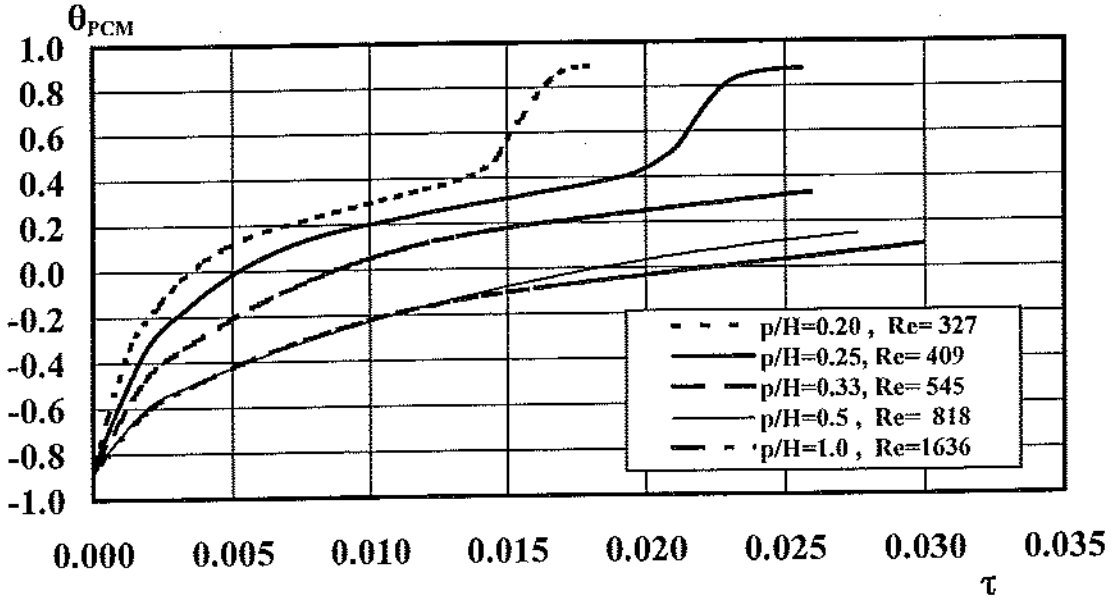

a) Average temperature of the PCM

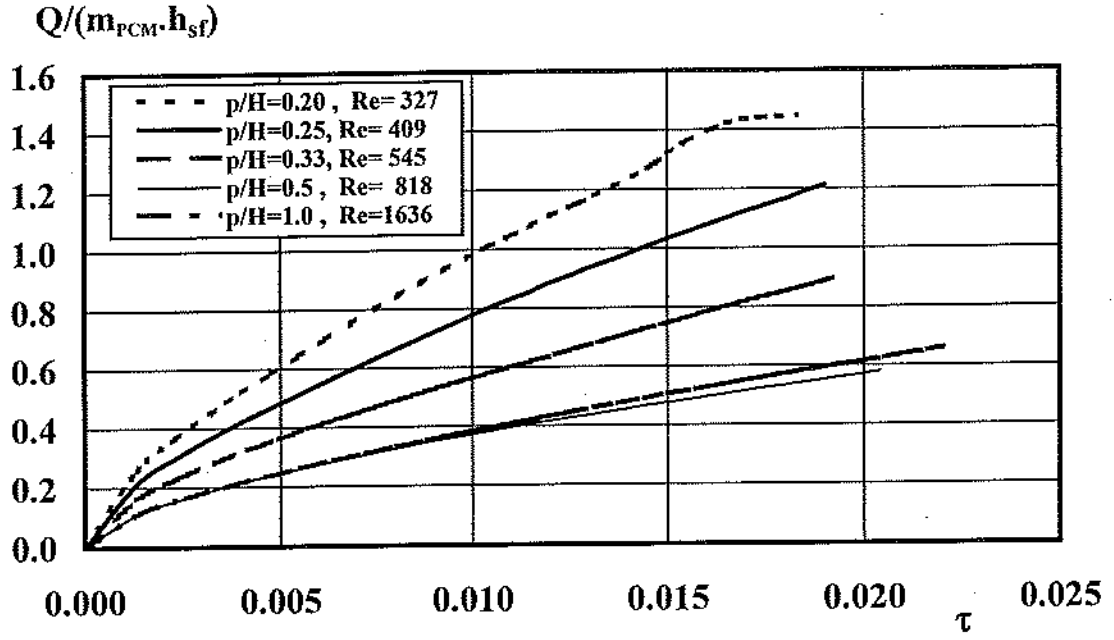

b) Heat storage

Fig.(8): Transient performance of storage units with the same storage volume and with different channel pitches operate at the same fluid mass flow rate (L/H=4.0, w/H=1.0, Ra=6.0×10^9, Ste=0.155 and Sc=0.18)

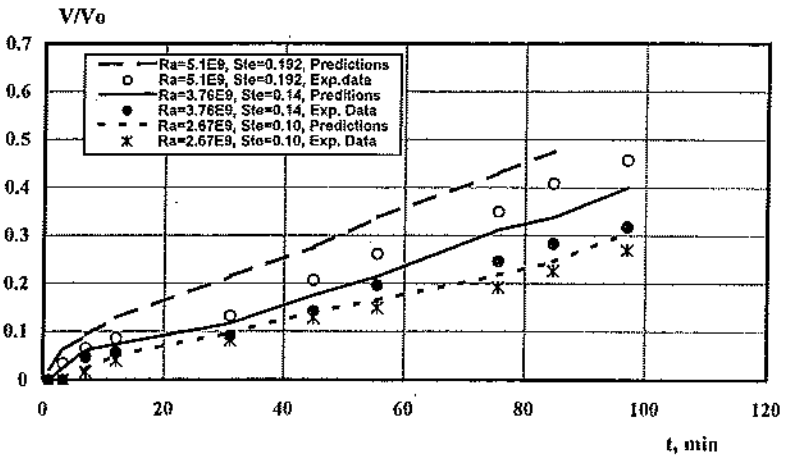

a) $Re_{DH} = 356$

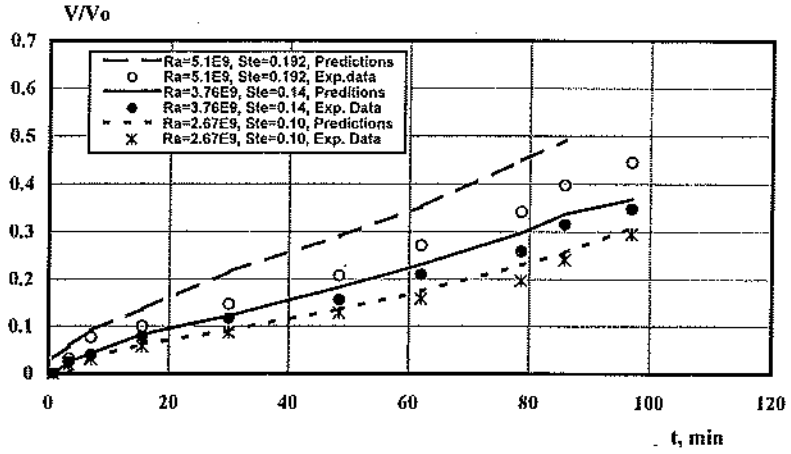

b) $Re_{DH} = 515$

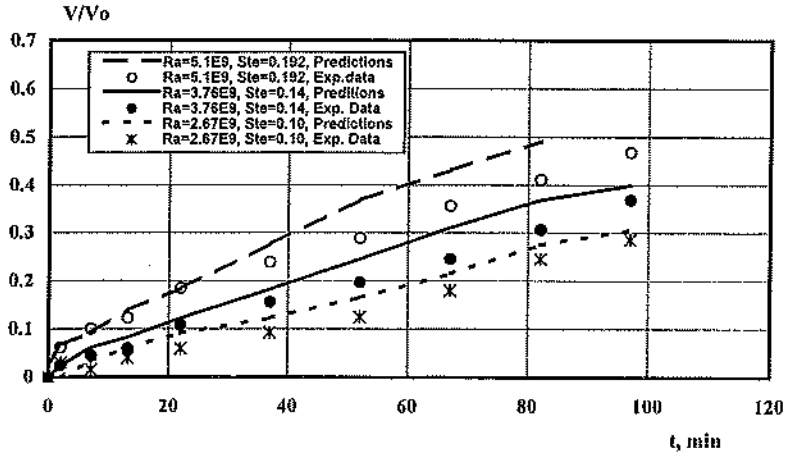

c) $Re_{DH} = 684$

Fig.(9): Temporal melted volume ratio for a storage unit with finned channels at different Reynolds numbers, (L/H=2.18, w/H=0.591, p/H=0.295 and S/L=0.281)

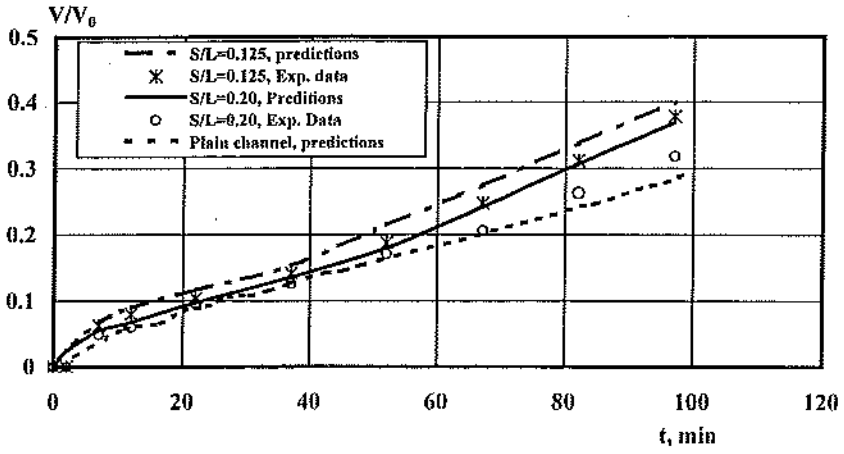

a) $Re_{DH} = 356$

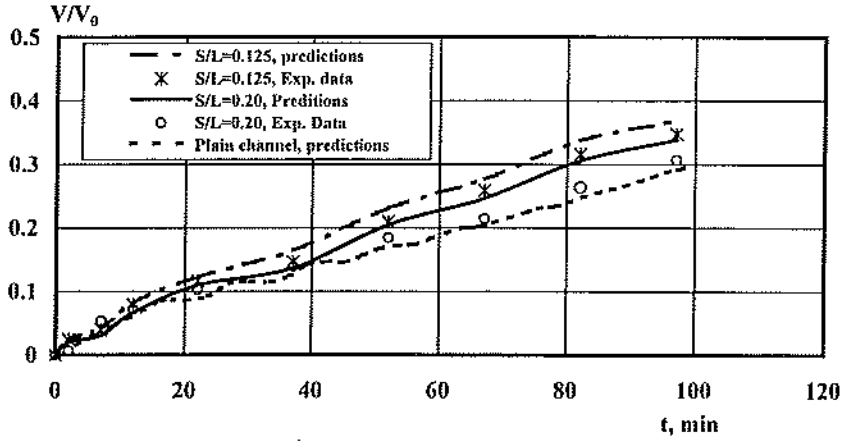

b) $Re_{DH} = 515$

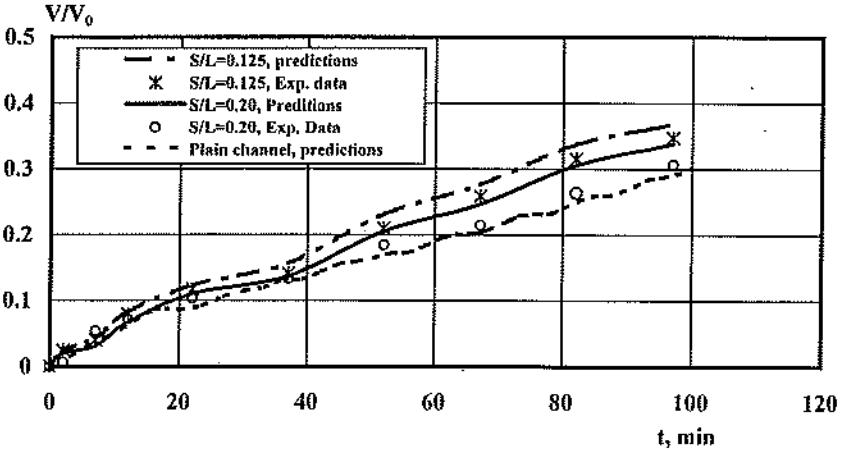

c) $Re_{DH} = 684$

Fig.(10): Performance enhancement due to the use of finned channels with different fin-pitches, ($Ra=3.76x10^9$, Ste=0.14, Sc=0.38, L/H=2.18, w/H=0.591and p/H=0.295)

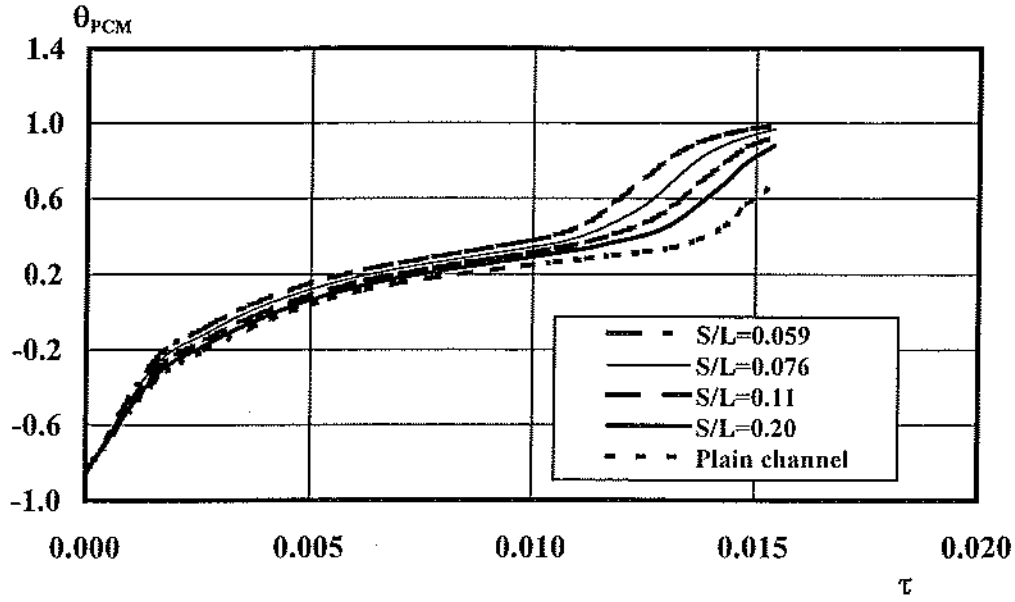

a) Average temperature of the PCM

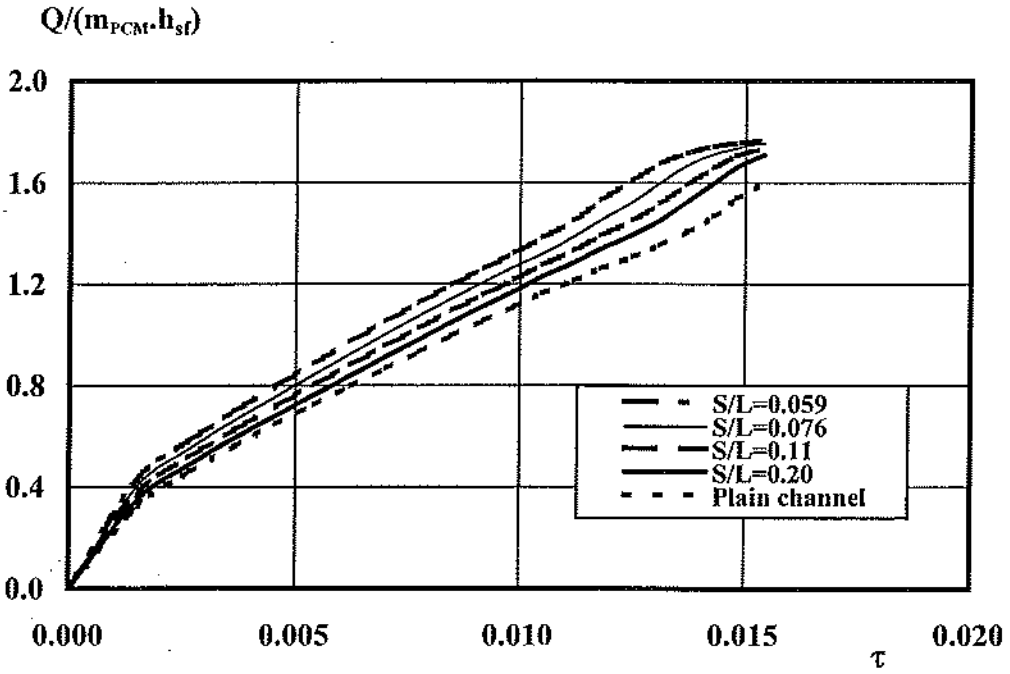

b) Heat storage

Fig.(11): Enhanced performance of a storage unit with finned channels at different fin pitch ratios: Enhanced model predictions at (l/p=0.163, t/p=0.0245, L/H=4.0, w/H=1.0, Ra=9.6×10^9, Ste=0.246, Re_{DH}=327 and Sc=0.18)

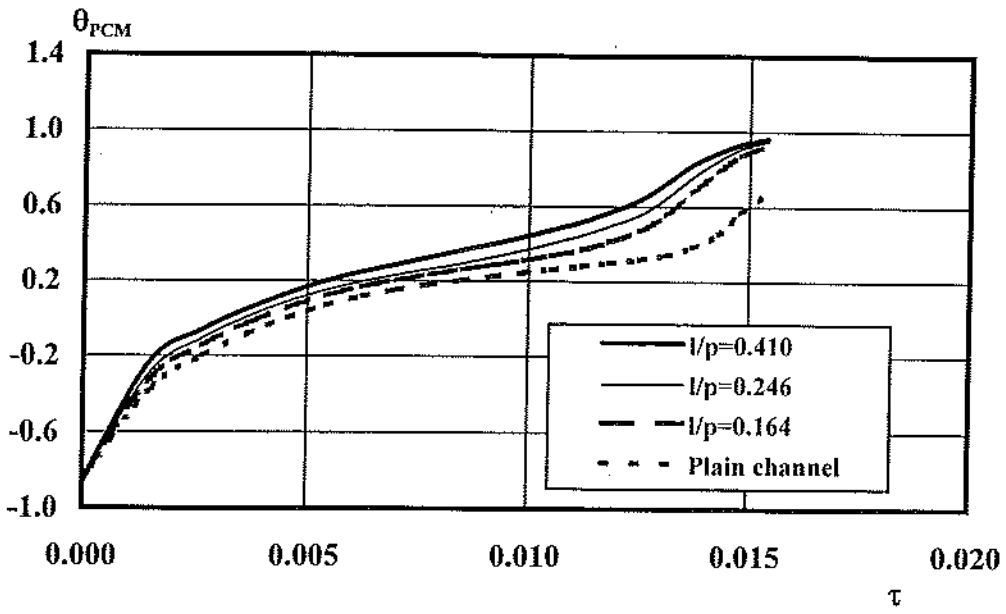

a) Average temperature of the PCM

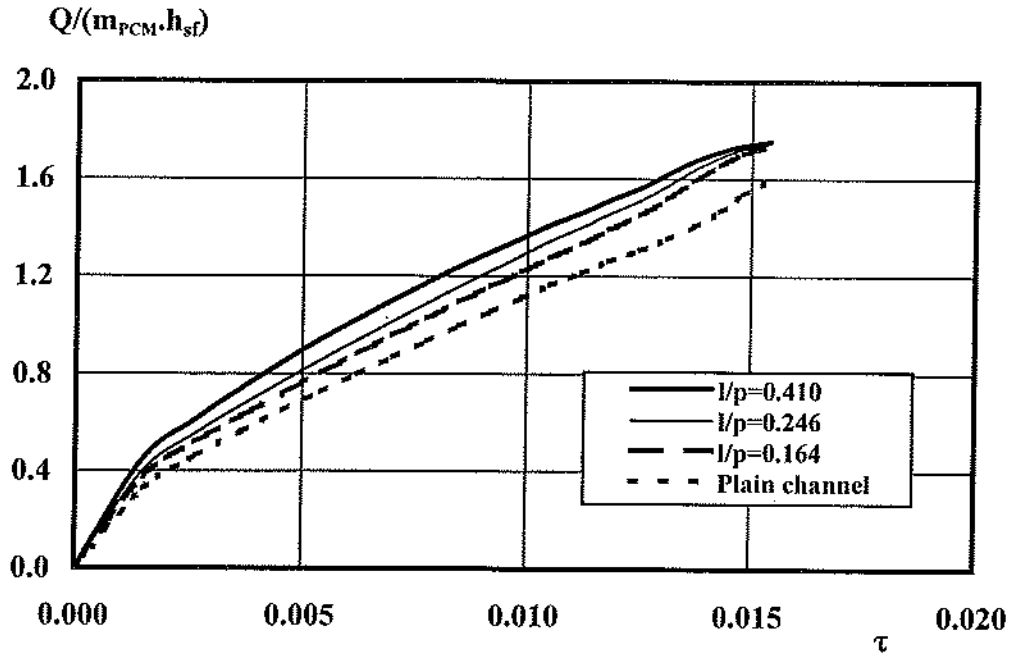

b) Heat storage

Fig.(12): Enhanced model predictions for storage unit with finned channels at different fin length ratios: (S/p=0.11, t/p=0.0245, L/H=4.0, w/H=1.0, $Ra=9.6x10^9$, Ste=0.246, Re_{DH}=327 and Sc=0.18)

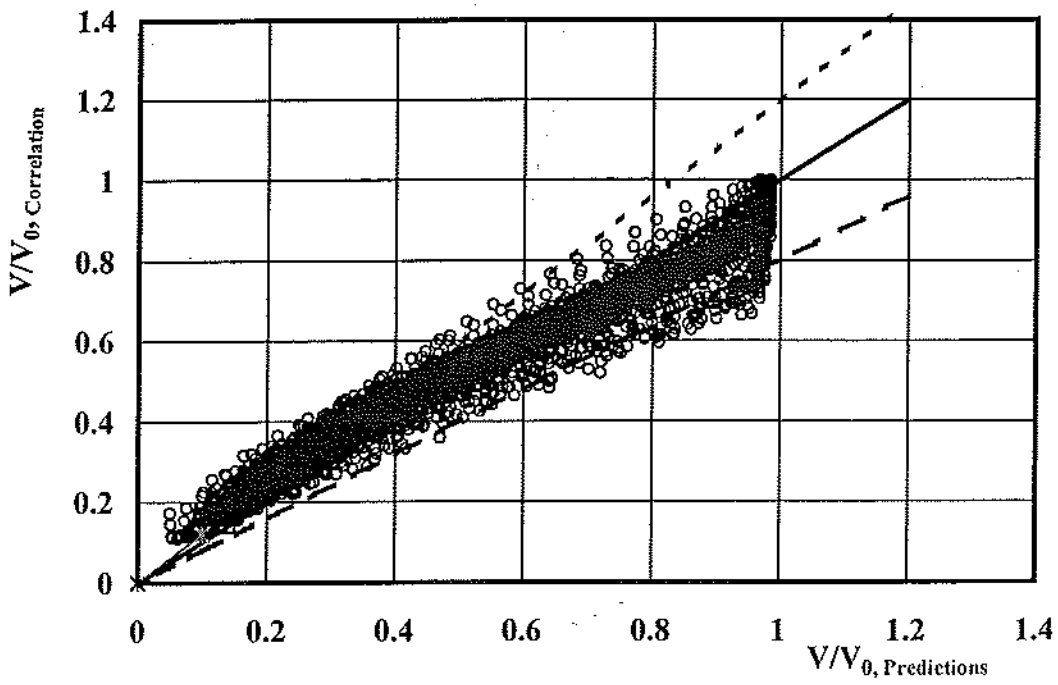

a) $Re_{DH} = 356$

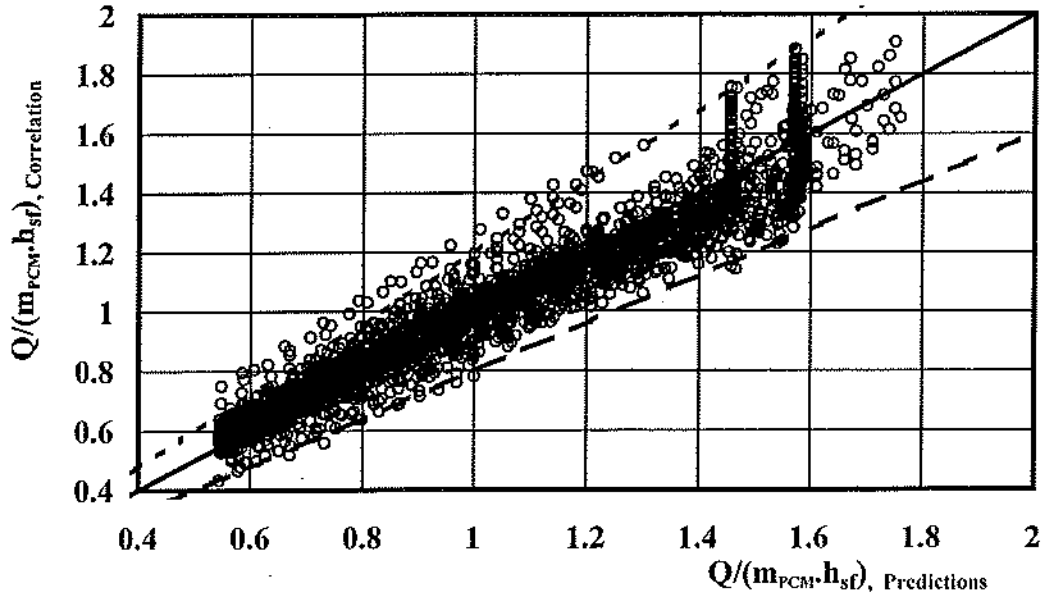

b) $Re_{DH} = 684$

Fig.(13): Validation of the present correlations via comparison with the present predictions

Session 3 : Energy II,III

Saturday 6 September 2003 1:40 PM – 5:00 PM
Session Chairman: Prof. Dr. Hany Moneib, Helwan University
20 Minutes per Presentation 10 minutes Discussions
(Session 3A : Energy II 1:40 – 3:10PM)

RAL-3-1. Life Cycle Energy Use of HVAC plant in Buildings: Optimization Replacement Cycles
David Arnold, Ph.D., Troup by Waters & Anders, Consulting Engineers, London, UK

RAL-3-2. Energy Efficiency, Merits, and Advantages of Various Air-Conditioning System in Commercial Buildings, In Egypt
Ramiz Kameel, Ph.D. and Essam E. Khalil, Member ASHRAE, Consultants, CEB, Cairo, Egypt

RAL-3-3. HVAC in Energy Efficiency Building Code, EEBC, Egypt
Essam E. Khalil, Chairman of National HVAC Code Committee , Egypt

Tea Break 3:10 - 3:30 PM
(Session 3B : Energy III 3:30 – 5:00PM)

RAL-3-4. Cooling Degree-Days for the Egyptian Climates
Al-Saied Khalil, PhD. Member ASHRAE.

RAL-3-5. Heat Transfer Enhancement in a Latent Heat Thermal Storage System Using Externally Finned Channels: Numerical and Experimental Study
K. M. El-Shazly, Professor, S. A. Abd El-Moniem, Atwan , Associate Professor , A. Abd El-Aziz.
K. K. Ali , Faculty of Eng. Shoubra, Benha Branch, Zagazig Univ., Cairo University, Egypt

RAL-3-6. Flow & Heat Transfer Enhancement in a Perforated Baffled HVAC Heat Exchanger
Reda Affify, Associate Professor, Faculty of Eng. Shoubra, Benha Branch, Zagazig Univ., Cairo University, Egypt Essam E. Mouguib, Research Student, Cairo University, Egypt
Mahmoud Fouad, Professor of Mechanical Engineering, Cairo University, Egypt

Session 4 : BACnet

Monday 8 September 2003 2:00 PM – 4:00 PM
Introducing BACnet interest group in Middle East .(BIG-ME)
Sabry An- Naggar and Vijay Kumar

President, ASHRAE Cairo Chapter

Dr. Alla Olama

Chairmen of the Scientific and Technical Committee

Prof. Dr. Mahmoud Fouad

ASHRAE

REGION-AT-LARGE

SECOND ANNUAL
REGIONAL CONFERENCE

CAIRO – EGYPT

SEPTEMBER 6th. – 8th. 2003

Hilton Pyramids Golf Resort –
the 6th of October City